



Correlation between micro-structural features and color of nanocrystallized powders of hematite

Morgane Gerardin, Nicolas Holzschuch, Alain Ibanez, Bernard Schmitt,
Pauline Martinetto

► To cite this version:

Morgane Gerardin, Nicolas Holzschuch, Alain Ibanez, Bernard Schmitt, Pauline Martinetto. Correlation between micro-structural features and color of nanocrystallized powders of hematite. AIC 2020 - Association Internationale de la Couleur / Couleur Naturelles - Couleurs Numériques, Nov 2020, Avignon, France. pp.1-7. hal-02975266

HAL Id: hal-02975266

<https://inria.hal.science/hal-02975266>

Submitted on 22 Oct 2020

HAL is a multi-disciplinary open access archive for the deposit and dissemination of scientific research documents, whether they are published or not. The documents may come from teaching and research institutions in France or abroad, or from public or private research centers.

L'archive ouverte pluridisciplinaire **HAL**, est destinée au dépôt et à la diffusion de documents scientifiques de niveau recherche, publiés ou non, émanant des établissements d'enseignement et de recherche français ou étrangers, des laboratoires publics ou privés.

Correlation between micro-structural features and color of nanocrystallized powders of hematite

Morgane Gerardin^{a,b,*}, Nicolas Holzschuch^a, Alain Ibanez^b, Bernard Schmitt^c, Pauline Martinetto^b

^a Univ. Grenoble Alpes, CNRS, Inria, Grenoble INP, LJK, 38000 Grenoble, France

^b Univ. Grenoble Alpes, CNRS, Institut Néel, 38000 Grenoble, France

^c Univ. Grenoble Alpes, CNRS, IPAG 38000 Grenoble, France

* Corresponding author: gerardin.morgane@gmail.com

Presenting author: Morgane Gerardin

ABSTRACT

Pigments are quite complex materials whose appearance involves many optical phenomena. Here, we focused on hematite as it is a traditional pigment, whose origin of coloration has been well discussed in the literature. Pure nanocrystallized α -Fe₂O₃ hematite powders have been synthesized using different synthesis routes. These powders have been characterized by X-ray powder diffraction and scanning electronic microscopy. The color of the samples has been studied by visible-NIR spectrophotometry. We obtained hematite with both various grain morphologies and noticeably different shades going from orange-red to purple. Colorimetric parameters in CIE L*a*b* color space and diffuse reflectance spectra properties were studied against the structural parameters. For small nanocrystals, hue is increasing with the grain size until a critical diameter of about 80 nm, where the trend is reversed. We believe a combination of multiple physical phenomena occurring at this scale may explain this trend.

Keywords: *hematite, pigment, reflectance, crystal structure*

INTRODUCTION:

Pigments are quite complex materials whose appearance involves many optical phenomena such as absorption and scattering. They are widely used in work of art and cosmetics among other things, for their coloring power. So, it is of great interest for digital representation to be able to predict the color of a pigment as a function of shape and size of its particles, or vice versa.

In this work, we have decided to focus on hematite as it is a traditional pigment, whose origin of coloration has been well discussed in the literature (Pailhé et al. (2008)). Moreover, we believe that this study can be adapted to any other inorganic pigment.

EXPERIMENTS

Synthesis of Hematite powders: As the preparation of hematite has been widely studied in the literature, it exists a lot of different routes to control the nucleation and growth of α -Fe₂O₃ crystallites in solution under standard or hydrothermal conditions. Our study has been done over thirteen samples, chosen to cover a wide range of morphologies and colors, and to mimic the color variations observed on archaeological rock paintings (Table 1).

Our samples numbered 1 to 6 have been respectively prepared following the *methods 1* to 6 described by Schwertmann et al. (2008). The samples 1₂ and 1₃ are obtained following the same route as 1 with adding an aging of one month after synthesis. The authors also propose a route to obtain *purple hematite*, but it resulted as goethite FeO(OH) which transformed to hematite after being annealed (here 16h at 270°C). It corresponds to the sample '*Annealed Goethite*' (AG). This production process is similar to the one of some hematite-based pigments used by Palaeolithic artists for rock paintings (Pomiès et al. (1998); Gialanella et al. (2011)). We generated peanuts-like hematite particles P₁ and P₂ following the routes proposed by Sugimoto et al. (1993). The sample HT has been prepared under hydrothermal conditions following the route of Sugimoto et al. (1993) for platelet particles. Finally, C is a commercial Iron(III) oxide powder sample purchased from Puratronic®.

Characterization: X-Ray powder diffraction (XRPD) data were collected on the dried powders with a Bruker Endeavour D8 diffractometer operated at Cu K α radiation ($\lambda = 1.5404 \text{ \AA}$). DIFFRAC.EVA's (Bruker) *search/match* module, which performs searches on the PDF4+ (2018) reference database, has been used for phase identification. All analyses of the X-ray powder diffraction patterns were performed with the FP_Suite softwares (Rodríguez-Carvajal, (1993)). Rietveld refinements (Rietveld, (1969)) were conducted to obtain the structural and micro-structural parameters of each powder and the mass proportion of hematite and goethite in case of mixture. Morphology (size and shape) of the grains composing the dried samples were studied by scanning electron microscopy (SEM, Zeiss Ultra+ microscope, Néel Institute, Grenoble, France).

The diffuse reflectance of the hematite powders was measured using the spectro-gonio radiometer SHADOWS developed by Potin et al. (2018). The measurements were performed on dried powder layer sample sufficiently thick so that the substrate does not contribute to the measured reflectance (>1mm), from 400nm to 1000nm with a step of 1 nm, with a normal incidence and an observation angle fixed at 30°. We used a Spectralon® as a white reference.

RESULTS AND DISCUSSION

XRPD: Hematite is identified in all of our samples (Figure 1). All samples are pure, except samples 5, 6 and HT, which contain a sufficiently small to be negligible amount of goethite (Figure 1 and Table 1). Crystallographic data and micro-structural parameters have been obtained from the Rietveld powder structure refinement analysis: unit cell parameters, atomic positions/occupancies and average crystallite size. Only the latter parameter seems to significantly

distinguish the different samples. It is calculated from the width of diffraction lines and corresponds to the size of domains over which diffraction is coherent. If the powder consists of single-crystals, crystallite size and grain size (entities seen under the microscope) are identical.

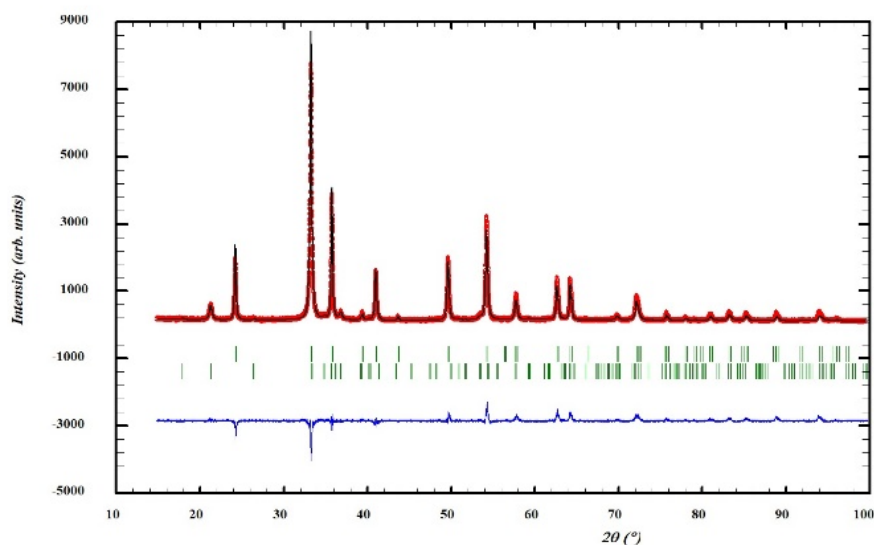


Figure 1: Rietveld refinement results (experimental pattern: red data points, calculated pattern: black full line, difference: blue full line) for samples 5. The vertical ticks indicate the Bragg positions for hematite and goethite respectively.

SEM: Except for 3 which is composed of two different size populations (a smaller one 3_s and a larger one 3_l), the monodispersity of all the samples is well controlled. Various shapes and sizes going from few nanometers to microns are observed (see Figure 2). *HT* is of big interest because this hexagonal platelet shape is quite similar to the morphology of some natural hematite-based pigment found in Lascaux's painting (Chalmin et al. 2004). 1 , 1_2 , 2 , 5 and 6 all show a diamond shape of different but nanometric sizes. The observed grains also differ from one another from their surface appearance: some of them such as P_1 , P_2 and 1_3 look quite rough. It may also be the case for 4 but the powder is too fine to confirm it. The description of the sample *C* is quite complex because it can be done at two different scales: small spheres seem to have been annealed so that they melted and assembled to form micrometric grains. The average dimensions of the grains were deduced from SEM images and reduced to only one dimensional parameter per sample by computing the radius of an equivalent sphere. In order to better take into account the shape anisotropy of certain samples (*AG* and *HT*), this radius has been computed so that the ratio of the surface over the volume of the grain remains constant. Results are listed in Table 1. Grain size and average crystallite size are in good agreement for all samples: it shows that the powders consist of single-crystals. Larger discrepancies are found for samples *AG*, *C*, P_1 and P_2 for which average crystallite size are very smaller than grain size. In this case, grains are therefore agglomerates of small single-crystals, as the SEM image of sample P_2 seems to show (Figure 2f).

Reflectance: As all of our samples are quite pure hematite, they all have the same spectral signature: in the studied wavelength range, hematite has three major absorption bands at around 600nm, 700nm and 850nm whose origins are

well described by Pailhé et al. (2008), and a fourth one near 430nm that is too saturated to be of such an interest. Depending on the sample under study, we either note a shift in wavelength, or a change of the intensity, the width and the slope of the bands (Figure 3). To achieve a colorimetric study and visualize the difference between the obtained colors, these spectra are converted into color coordinates in the CIE $L^*a^*b^*$ space.

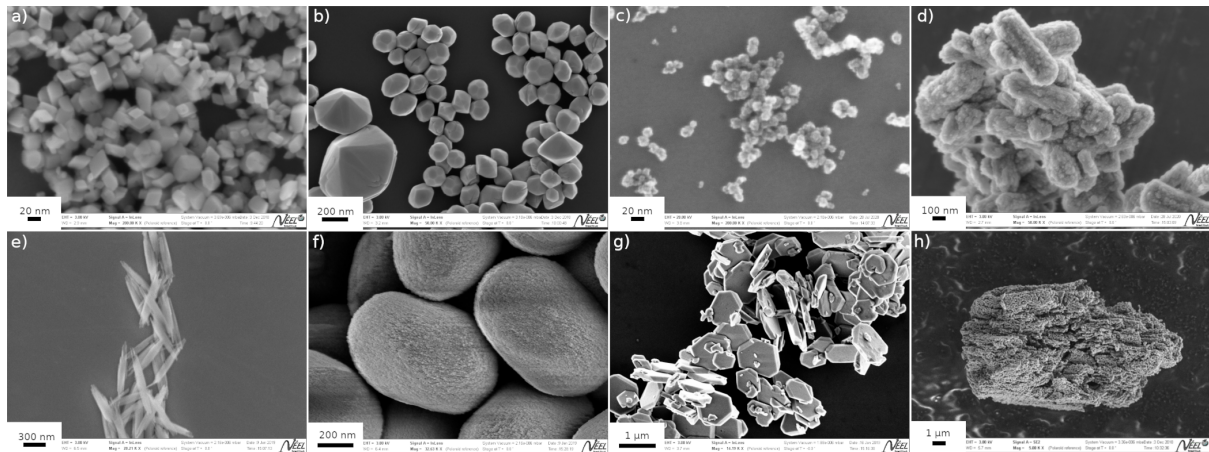
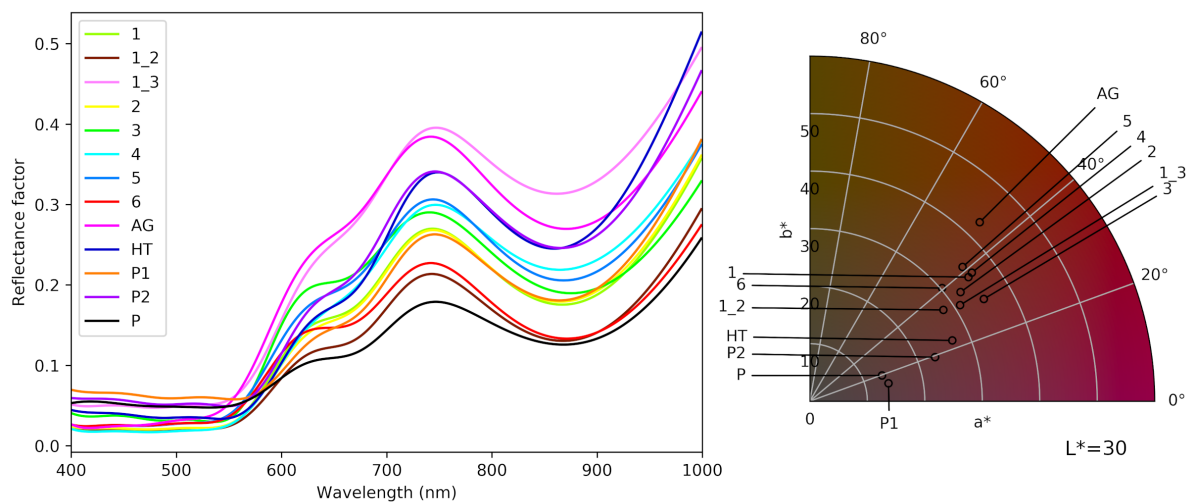


Figure 2: SEM images of the different hematite powders. a) Crystals of samples 1, 1₂, 2, 5 and 6 show pretty similar morphology: same diamond shape and close sizes. Only 1 is shown here. b) Sample 3 presents two bi-pyramid shaped crystal populations different in size. c) Sample 4 is composed of very small spherical particles. d) Sample 1₃ consists of crystals with a rough surface e) Sample AG (flat needle shape whose thickness is much smaller than its width and its length). f) Samples P₁ and P₂ have the same shape and different sizes. They seem to consist of agglomerates of crystals, forming grains. Only P₂ is shown here. g) Sample HT (large-sized hexagonal platelet shape). h) Sample C presents sticks composed of melted spheres of much smaller size.



*Figure 3: Reflectance spectra of the samples, calibrated by a Spectralon®, and position of the corresponding colors in the CIE $L^*a^*b^*$ diagram for $L^*=30$.*

The thirteen syntheses of hematite lead to crystals (or agglomerates of crystals) with different morphologies and/or sizes and to as many powders of different colors that are summarized in Table 1. The micro-structural parameters, spectra characteristics and color parameters have been studied alongside with each other to find a correlation between them. In every case, it is possible to distinguish different trends for the very small particles (<80 nm in diameter) and the bigger ones. The most striking results are obtained for the study of the hue against the grain sizes (see Figure 4). The hue, defined as the angular component of the color in the polar representation (see Figure 3), is first increasing for small particles, then the trend is reversed after reaching a critical diameter (~80nm).

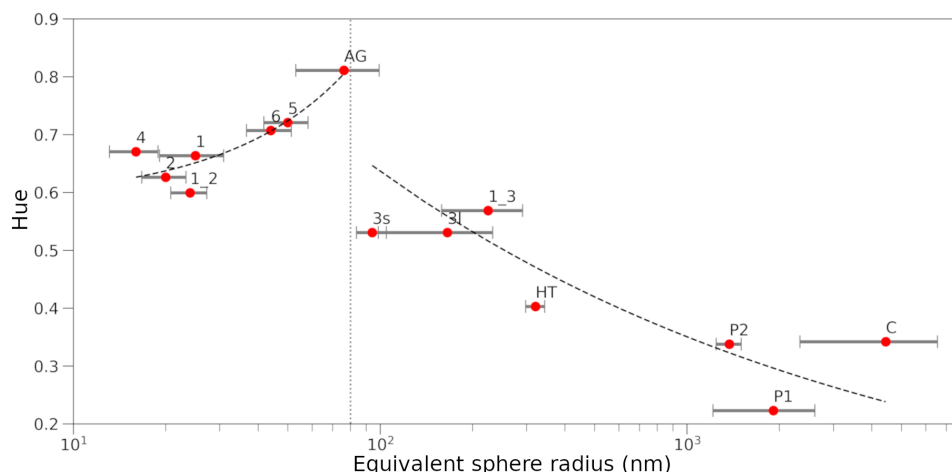


Figure 4: Hue against the equivalent sphere diameter deduced from SEM experiments. The hue is increasing for very small particles until a critical diameter (~80nm, dot line)) where the trend is reversed.














Numerous physical phenomena depending on the grain size that are at stake and becoming predominant over one another at this scale should be the cause of such a trend, absorption and scattering being the more important. Simulations of different scattering models are underway in order to fit the reflectance spectra, using numerous phase functions such as Rayleigh, Mie or Henyey-Greenstein. (Bohren and Huffman (1983), Henyey and Greenstein (1941)). To faithfully describe the observed color of the powders, a precise measure of the hematite refractive index would be necessary. As far as we know, only one measurement of this index has been done by Querry (1985), and not any other ever since.

CONCLUSION

Thirteen nanocrystallized hematite powders showing various morphologies and/or sizes of crystals (or agglomerates of crystals) and a wide range of colors have been synthesized. By comparing the micro-structural features, the characteristics of measured reflectance spectra and the color parameters in the CIE L^*a^*b space, it has been observed that some parameters are highly correlated. The study of the hue versus the grain size of the powders shows that the trend following by these parameters is reversed when reaching a critical diameter of about 80nm. We believe that the influence of different scattering phenomena at stake is changing at this scale causing this change of trend.

Simulations of reflectance spectra with well described scattering models are needed to correctly understand the color of each sample according to the grain size and shape. An accurate measure of the refractive index would be useful to produce more reliable results. We will also aiming to model the bi-directional reflectance distribution function (BRDF), that would be of great interest for digital representation.

In the future we would like to extend this study to other inorganic pigments, like ochers, mixtures of hematite and clay.

	Grain shape	Grain size (nm)	Average crystallite size (nm) ± anisotropy	Goethite (%m)	Color (L*a*b*)	
4	Sphere	16.0 ± 2.88	10.9 ± 0.40		(27.1, 28.2, 22.3)	
2	Diamond	20.0 ± 3.28	20.1 ± 3.00		(27.2, 26.2, 19.0)	
1 ₂	Diamond	24.0 ± 3.22	25.4 ± 4.90		(25.0, 23.2, 15.9)	
1	Diamond	25.0 ± 5.90	24.5 ± 4.80		(27.5, 27.6, 21.6)	
6	Diamond	44.0 ± 7.40	61.2 ± 10.2	7.17 ± 0.18	(29.6, 23.0, 19.7)	
5	Diamond	50.0 ± 8.20	46.3 ± 8.80	8.98 ± 0.16	(31.4, 26.6, 23.3)	
AG	Needle	76.2 ± 23.2	7.30 ± 3.60		(36.2, 29.6, 31.1)	
3	Bi- pyramid	94.2 ± 10.5 166 ± 67.0	197 ± 50.8		(32.4, 30.3, 17.8)	
1 ₃	Stick	224 ± 66.2	206 ± 43.2		(36.2, 26.1, 16.7)	
HT	Platelet	320 ± 22.8	399 ± 242	0.91 ± 0.09	(29.3, 24.8, 10.6)	
P ₂	Ellipsoid	1374 ± 128	18.3 ± 0.40		(32.7, 21.8, 7.65)	
P ₁	Ellipsoid	1914 ± 698	16.6 ± 2.30		(32.1, 13.7, 3.10)	
C	Sphere or stick	98.0 ± 25.0 4444 ± 2108	526 ± 53.3		(29.7, 12.6, 4.47)	

*Table 1: Features of the hematite crystals (or agglomerates of crystals) and colors of the powders. The samples have been organized by increasing crystallite size). Grain shapes and sizes are determined through SEM images. Average crystallite sizes and mass proportions of goethite are optimized through Rietveld refinements. Colors are calculated from the reflectance spectra in the CIE L*a*b* color space.*

ACKNOWLEDGEMENTS

The authors would like to thank S. Pairis, S. Giraud (Insitut Néel) for their help in the manipulation of the scanning electron microscope, and the chemical syntheses respectively, as well as C. Félix (Institut Néel) and O. Brissaud (IPAG) for their help in the reflectance measurements. This work was financially supported *by the*

French National Research Agency in the framework of the Investissements d'Avenir program (**ANR-15-IDEX-02**, Cross Disciplinary Program Patrimialp).

REFERENCES

- Bohren, Craig F., and Donald R. Huffman. "Absorption and scattering of light by small particles". John Wiley & Sons, 2008.
- Chalmin, Emilie, Michel Menu, Marie-Pierre Pomiès, Colette Vignaud, Norbert Aujoulat, and Jean-Michel Geneste. "Les blasons de Lascaux." *L'anthropologie* 108, no. 5 (2004): 571-592.
- Gialanella, Stefano, R. Belli, G. Dalmeri, I. Lonardelli, M. Mattarelli, M. Montagna, and L. Toniutti. "Artificial or natural origin of Hematite-based red pigments in archaeological contexts: the case of Riparo Dalmeri (Trento, Italy)." *Archaeometry* 53, no. 5 (2011): 950-962.
- Heney, Louis G., and Jesse L. Greenstein. "Diffuse radiation in the galaxy." *The Astrophysical Journal* 93 (1941): 70-83.
- Pailhé, Nathalie, Alain Wattiaux, Manuel Gaudon, and Alain Demourgues. "Correlation between structural features and vis-NIR spectra of α -Fe₂O₃ hematite and AFe₂O₄ spinel oxides (A= Mg, Zn)." *Journal of Solid State Chemistry* 181, no. 5 (2008): 1040-1047.
- Pailhé, Nathalie, Alain Wattiaux, Manuel Gaudon, and Alain Demourgues. "Impact of structural features on pigment properties of α -Fe₂O₃ haematite." *Journal of Solid State Chemistry* 181, no. 10 (2008): 2697-2704.
- Pomies, Marie-Pierre, Guillaume Morin, and Colette Vignaud. "XRD study of the goethite-hematite transformation: application to the identification of heated prehistoric pigments." *European Journal of solid state and Inorganic Chemistry* 35, no. 1 (1998): 9-25.
- Potin, Sandra, Olivier Brissaud, Pierre Beck, Bernard Schmitt, Yves Magnard, Jean-Jacques Correia, Patrick Rabou, and Laurent Jocu. "SHADOWS: a spectro-gonio radiometer for bidirectional reflectance studies of dark meteorites and terrestrial analogs: design, calibrations, and performances on challenging surfaces." *Applied optics* 57, no. 28 (2018): 8279-8296.
- Querry, Marvin R. *Optical constants*. MISSOURI UNIV-KANSAS CITY, 1985.
- Rietveld, Hugo M. "A profile refinement method for nuclear and magnetic structures." *Journal of Applied Crystallography* 2 (1969): 65-71.
- Rodríguez-Carvajal, Juan. "Recent advances in magnetic structure determination by neutron powder diffraction." *Physica B* 192, no. 1-2 (1993): 55-69.
- Schwertmann, Udo, and Rochelle M. Cornell. *Iron oxides in the laboratory: preparation and characterization*. John Wiley & Sons, 2008.
- Sugimoto, Tadao, Mohammad M. Khan, and Atsushi Muramatsu. "Preparation of monodisperse peanut-type α -Fe₂O₃ particles from condensed ferric hydroxide gel." *Colloids and Surfaces A: Physicochemical and Engineering Aspects* 70, no. 2 (1993): 167-169.
- Sugimoto, Tadao, Atsushi Muramatsu, Kazuo Sakata, and Daisuke Shindo. "Characterization of hematite particles of different shapes." *Journal of colloid and interface science* 158, no. 2 (1993): 420-428.